Journal of Crohn's and Colitis, 2018, 217–229
doi:10.1093/ecco-jcc/jjx115
Advance Access publication August 18, 2017
Original Article

Original Article

Oral Delivery of Nanoparticles Loaded With Ginger Active Compound, 6-Shogaol, Attenuates Ulcerative Colitis and Promotes Wound Healing in a Murine Model of Ulcerative Colitis

Mingzhen Zhang,[a,#] Changlong Xu,[a,c,#] Dandan Liu,[d] Moon Kwon Han,[a] Lixin Wang,[a,b] Didier Merlin[a,b]

[a]Institute for Biomedical Sciences, Georgia State University, Atlanta, GA, USA [b]Atlanta Veterans Affairs Medical Center, Decatur, GA, USA [c]Department of Gastroenterology, 2nd Affiliated Hospital and Yuying Children's Hospital of Wenzhou Medical University, Zhejiang, P. R. China [d]Department of Chemistry, Georgia State University, Atlanta, GA, USA

[#]These authors contributed equally to this work.

Corresponding author: Mingzhen Zhang, Institute for Biomedical Sciences, Center for Diagnostics and Therapeutics, Georgia State University, Atlanta, GA 30302, USA. Tel.: +1 [404] 413 3597; fax: +1 [404] 413 3580; email: mzhang21@gsu.edu

Abstract

Background and Aims: Oral drug delivery is the most attractive pathway for ulcerative colitis [UC] therapy, since it has many advantages. However, this strategy has encountered many challenges, including the instability of drugs in the gastrointestinal tract [GT], low targeting of disease tissues, and severe adverse effects. Nanoparticles capable of colitis tissue-targeted delivery and site-specific drug release may offer a unique and therapeutically effective system that addresses these formidable challenges.

Methods: We used a versatile single-step surface-functionalising technique to prepare PLGA/PLA-PEG-FA nanoparticles loaded with the ginger active compound, 6-shogaol [NPs-PEG-FA/6-shogaol]. The therapeutic efficacy of NPs-PEG-FA/6-shogaol was evaluated in the well-established mouse model of dextran sulphate sodium [DSS]-induced colitis.

Results: NPs-PEG-FA exhibited very good biocompatibility both *in vitro* and *in vivo*. Subsequent cellular uptake experiments demonstrated that NPs-PEG-FA could undergo efficient receptor-mediated uptake by colon-26 cells and activated Raw 264.7 macrophage cells. *In vivo*, oral administration of NPs-PEG-FA/6-shogaol encapsulated in a hydrogel system [chitosan/alginate] significantly alleviated colitis symptoms and accelerated colitis wound repair in DSS-treated mice by regulating the expression levels of pro-inflammatory [TNF-α, IL-6, IL-1β, and iNOS] and anti-inflammatory [Nrf-2 and HO-1] factors.

Conclusions: Our study demonstrates a convenient, orally administered 6-shogaol drug delivery system that effectively targets colitis tissue, alleviates colitis symptoms, and accelerates colitis wound repair. This system may represent a promising therapeutic approach for treating inflammatory bowel disease [IBD].

Key Words: Ulcerative colitis; drug delivery system; therapy

1. Introduction

Inflammatory bowel diseases [IBDs], which include Crohn's disease [CD] and ulcerative colitis [UC], are chronic debilitating inflammatory conditions.[1,2] The conventional therapies currently used to treat IBD patients can fall into three groups: anti-inflammatory medications [such as aminosalicylates and corticosteroids], immunosuppressants, and antibiotics.[3–5] These medications can temporarily induce and maintain remission, but 80% and 45% of CD and UC patients, respectively, will require at least one surgical intervention in their lifetimes.[6,7]

Conventional oral formations [eg pellets, capsules, or tablets] are of limited use in IBD. These approaches, which are generally designed to achieve systemic delivery of therapeutics, can have many drawbacks including inefficacy, ineffective control of drug release, therapeutic variation due to IBD symptoms [eg diarrhoea and a modified colonic environment], and limit targeting of inflamed areas. Furthermore, the enhanced permeability that characterises the intact non-inflamed tissues of the upper intestinal tract in patients with IBD may mean that such drugs can have serious adverse effects.[8] Therefore, we need to develop novel carrier systems capable of delivering drugs specifically and exclusively to the inflamed regions associated with this disease.[9,10]

Among the novel carrier systems introduced in recent years, nanoparticles [NPs]-based drug-delivery systems [DDSs] are promising carriers for improving IBD therapy. Various DDSs [ie liposomes, mesoporous silica, and polymer NPs] have been rationally designed to be orally administered, release a loaded drug at a specific pH value, resist digestive enzymes, and/or require bacterial cleavage for activation.[11–14] In general, these DDSs provide several substantial advantages over the conventional methods, such as by protecting the loaded drug against environmental degradation, improving drug solubility, enhancing absorption, and enabling sustained drug release.[15,16] An NP-based delivery system can help the loaded drug specifically to accumulate at inflamed tissues, due to the increased permeability of such tissues. Furthermore, certain cell receptors or transporters that are over-expressed during the inflammatory response, such as CD44,[17] CD98,[18,19] and folate receptor,[20,21] can be exploited for active drug targeting.[22]

Ginger [*Zingiber officinale* Roscoe] has been widely used as a spice, dietary supplement, and traditional medicine for centuries.[23–25] We recently demonstrated that a specific population of ginger-derived NPs may effectively reduce colitis,[26–29] and showed that the major pharmacologically active compounds of these ginger NPs may be gingerols and shogaols. 6-shogaol, which is a major component of dried ginger, has received much attention because it has antioxidative, anti-inflammatory, and anticarcinogenic properties,[30,31] and shows superior biological activity and enhanced stability compared with its counterpart in fresh ginger extract. However, it is not yet known whether 6-shogaol could have therapeutic efficacy against UC.

In this study, we prepared folate-functionalised 6-shogaol loaded PLGA/PLA NPs [NPs-PEG-FA/6-shogaol] using a versatile single-step surface-functionalising technique [as shown in Figure 1A]. We first characterised their physicochemical properties [morphology, particle size, zeta potential, and drug release profile] and further evaluated their biocompatibility both *in vitro* and *in vivo*. Subsequent cellular uptake experiments demonstrated that NPs-PEG-FA could undergo efficient receptor-mediated uptake by colon-26 cells and activated Raw 264.7 macrophage cells. Our *in vivo* results showed that oral administration of NPs-PEG-FA/6-shogaol in a hydrogel system [chitosan/alginate] significantly alleviated colitis symptoms and accelerated colitis wound repair in DSS-treated colitic mice, by regulating the expression levels of pro-inflammatory [TNF-α, IL-6, IL-1β, and iNOS] and anti-inflammatory [Nrf-2 and HO-1] factors. This novel system may represent a promising therapeutic approach for treating IBD.

2. Methods

2.1. Materials

Lactide:glycolide [75:25] [PLGA], molecular weight 66 000–107 000, poly [vinyl alcohol] [PVA, 86–89% hydrolyzed, low molecular weight], 6-shogaol, and its analysis standard, phalloidin-FITC, were purchased from Sigma [St. Louis, MO, USA]. PLA-PEG and PLA-PEG FA [PEG MW 5000 and PLA MW 10000] were obtained from NSP-Functional polymers and copolymers [Winston-Salem; NC, USA]. Fluorescent lipophilic dyes, 1, 1'-dioctadecyl-3,3,3',3'-tetramethylindocar-bocyanine perchlorate [DiL] and 1,1'-dioctadecyl-3,3',3'- tetramethylindotricarbocyanine iodide [DiR], were purchased from Promokine [Heidelberg, Germany]. FITC-Annexin V/propidium iodide [PI] apoptosis kit was purchased from BD biosciences [San Jose, CA, USA]. XenoLight RediJect Chemiluminescent Inflammation Probe was purchased from PerkinElmer [Waltham, MA, USA]. Lipocalin-2 duoset enzyme-linked immunosorbent assay [ELISA] kit was purchased from RandD Systems [Minneapolis, MN, USA]. FR Antibody [FL-257] was obtained from Santa Cruz [Dallas, TX, USA].

2.2. Preparation of NPs

To prepare ginger active compound 6-shogaol loaded NPs-PEG-FA nanoparticles, PLGA [75 mg] and 6-shogaol (6 mg, 25 µL dimethyl sulphoxide [DMSO]) were dissolved in 2 mL of dichloromethane [DCM]. An oil-in-water emulsion was formed by emulsifying the polymer solution in 4 mL of 2.5 % w/v aqueous polyvinyl alcohol [PVA] solution using probe sonicator at 50% amplitude for 2 min [Branson S-450; Danbury, CT, USA] over an ice bath; 25 mg of PLA-PEG/PLA-PEG-FA mix with different PLA-PEG-FA amounts of 10 mg [as NPs-PEG-FA-1], 15 mg [as NPs-PEG-FA-2], and 20 mg [as NPs-PEG-FA-3] were dissolved in DCM [200 µL] and added dropwise to the above emulsion with stirring. The emulsion was stirred overnight at room temperature, followed by 2 h of rotary evaporation under vacuum to remove the residual DCM. Nanoparticles were recovered by centrifugation [15 000 rpm, 15 min, at 4°C] and washed three times with de-ionised water. NPs suspension was then lyophilised to obtain a dry powder. DiL- or DiR-loaded nanoparticles involved the same procedures.

2.3. Characterisation of NPs

The particle size and zeta potential of NPs-PEG and NPs-PEG-FA were determined using a Malvern Zetasiser Nano ZS90 Apparatus [Malvern Instruments, Malvern, UK] at room temperature. The morphology of NPs-PEG and NPs-PEG-FA was obtained using transmission electron microscopy [TEM].

High performance liquid chromatography [HPLC] analysis was performed to evaluate 6-shogaol loading efficiency using an Agilent® 1100 LC System [Agilent Technologies Inc.; CA, USA]. The system was optimised in order to reduce dead volume and improve performance including: increasing the UV scan rate; changing the injector needle seat; re-plumbing the system with red PEEKsil™ Tubing [SGE]; and using a semi-micro flow cell. The C18 column was from Phenomenex [Torrance, CA, USA]. All samples were dissolved in

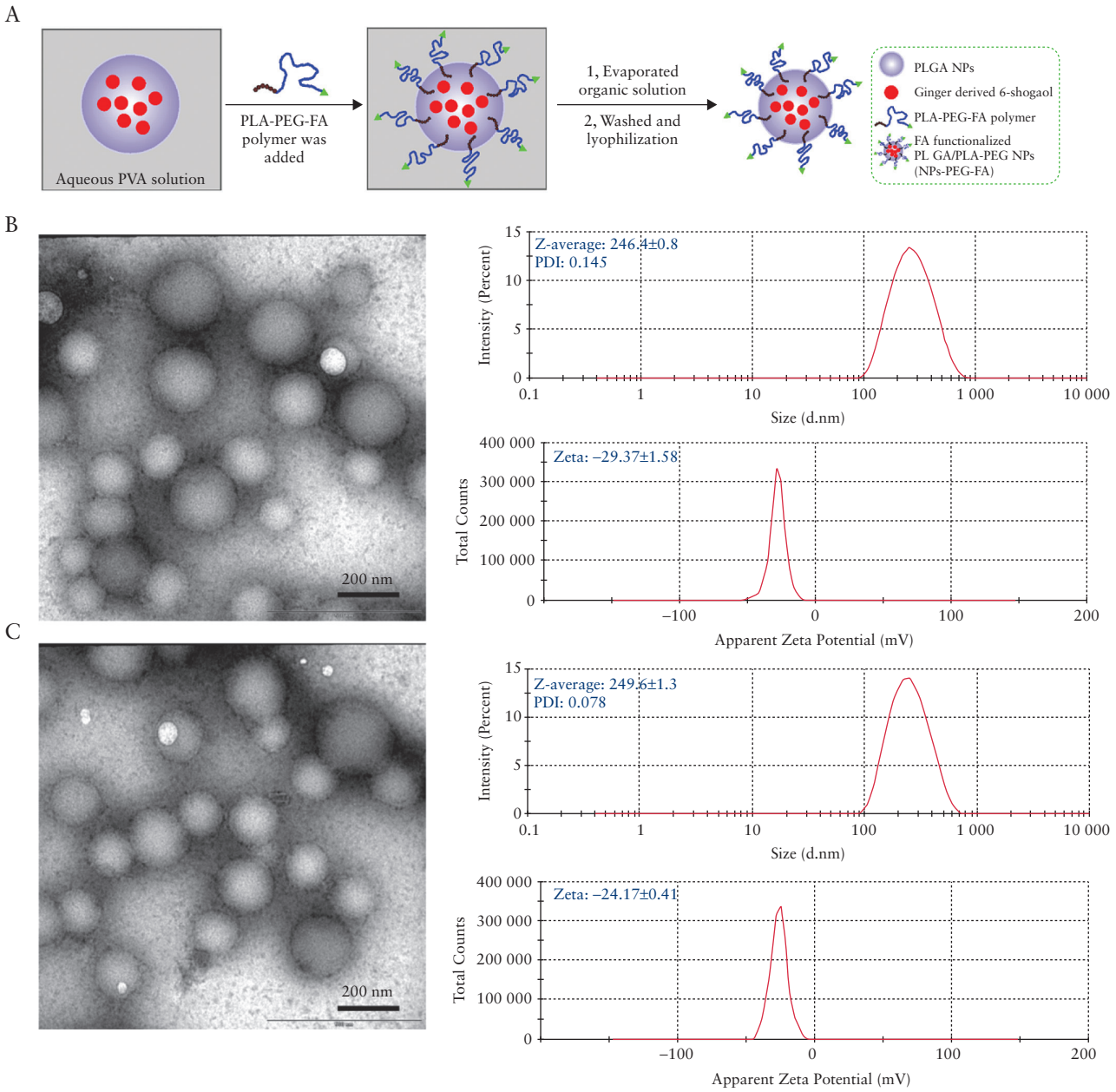

Figure 1. Preparation and characterisation of 6-shogaol loaded polymeric nanoparticles. A: Schematic illustration of process through which PLGA/PLA-PEG-FA nanoparticles [NPs-PEG-FA] were fabricated using a versatile single-step surface-functionalising technique. B: The morphology of PLGA/PLA-PEG nanoparticles [NPs-PEG] was characterised by transmission electron microscopy [TEM], and their size and zeta potential were measured by dynamic light scattering [DLS] using a Malvern Zetasizer Nano ZS90 Apparatus. C: The morphology, size, and zeta potential of PLGA/PLA-PEG-FA [NPs-PEG-FA] were characterised.

methanol/water [80:20] with 0.1 % trifluoroacetic acid [TFA] added as a stabiliser. Before injection, samples were filtered through a 0.45-µm syringe filter. The detection wavelength was set at 282 nm.

The release kinetics of 6-shogaol from NPs were carried out using Slide-A-Lyzer mini dialysis devices [MW 20k]. Briefly, 10 mg of NPs-PEG or NPs-PEG-FA were dispersed in 10 mL phosphate-bufferef saline [PBS] [pH 7.0]. The samples were shaken at 200 rpm at room tempreature. Aliquots were taken out from the dialysis bag at spectified time points [0, 4, 8, 24, 48, and 72 h], and the release of 6-shogaol from NPs into the buffer solution was monitored via the HPLC method.

2.4. Cell lines and cultures

Raw 264.7 macrophage and colon-26 cells were cultured to confluence in 75-cm^2 flasks at 37°C in a humidified atmosphere containing 5% CO_2. Raw 264.7 macrophage cells were cultured in Dulbecco's Modified Eagle Medium [DMEM], and colon-26 cells were cultured in RPMI 1640 medium [Life Technologies; NY, USA]. Media were supplemented with penicillin [100 U/mL], streptomycin [100 U/mL], and heat-inactivated fetal bovine serum [10 %] [Atlanta Biologicals; GA, USA]. The activation of macrophages was optimised using different doses of lipopolysaccharide [LPS] [2 ng/mL and 500 ng/mL], different incubation times [4 h, 12 h, and 24 h], and cultivation of

cells in either normal DMEM growth medium or folate-free DMEM medium. For *in vitro* experiments, following the optimisation of conditions, cells were activated with 500 ng/mL LPS for 12 h, unless otherwise stated.

2.5. Biocompatibility assays

MTT cell proliferation assay was first used to analysis the effect of NPs on cell viability of Raw 264.7 macrophage and colon-26 cells. Briefly, cells were seeded in 96-well plates at a density of 1×10^4 cells/well, and incubated overnight. Different concentrations of PLGA NPs, NPs-PEG, and NPs-PEG-FA [50, 100, 200, 500, 1000 μg/mL] were added to the plate and incubated for 24 h and 48 h. Then, 20 μL/well of MTT solution [5 mg/mL in PBS] were added to each well and incubated for another 4 h. Finally, the plates were shaken thoroughly for 1 min on the shaker, and absorbance was measured at 480 nm using a microplate reader.

To evaluate the biocompatibility of NPs-PEG-FA *in vivo*, mice underwent oral administration of NPs-PEG-FA [15 mg in PBS] or PBS [control] for 7 days. Body weight changes, blood, different parts of intestinal tract [stomach, duodenum, jejunum, ileum, and colon] and main organs [heart, liver, spleen, lung, and kidney] were collected to compare with control. Blood cells and biochemical analyses were performed using a haematology analyser [VetScan HM5; Abaxis, CA, USA] and a biochemical analyser [[VetScan VS2; Abaxis, CA, USA], respectively.

2.6. Cellular uptake of NPs-PEG-FA *in vitro*

The experiment was carried out using DiL-loaded NPs-PEG-FA [NPs-PEG-FA/DiL] to analyse the cellular uptake of these nanoparticles by fluorescence microscopy imaging. Colon-26 cells and activated Raw 264.7 macrophage cells with the concentration of 1×10^5/well were seeded in eight-chamber tissue culture glass slides [Tissue-Tek; Sakura, USA] overnight. NPs-PEG/DiL and NPs-PEG-FA/DiL were incubated with cells for 6 h. Then the cells were fixed with 4 % paraformaldehyde [PFA] for 15 min, and dehydrated with acetone at -20°C for 5 min. After blocking with 1% bovine serum albumen [BSA] in PBS for 30 min, 100 μL of phalloidin-FITC [1:40 dilution] was added and the mixture was incubated for an additional 30 min. Finally, cells were coverslip-mounted with mounting medium containing 4-, 6-diamidino-2-phenylindole [DAPI]. Images were observed using an Olympus fluorescence microscopy equipped with a Hamamatsu Digital Camera ORCA-03G.

2.7. Comparison of cellular uptake efficiency by flow cytometry

Colon-26 cells and activated Raw 264.7 macrophage cells with the concentration of 1×10^5/well were seeded in six-well plates and incubated overnight. Cells were treated with NPs, NPs-PEG, NPs-PEG-FA-1, NPs-PEG-FA-2, and NPs-PEG-FA-3, respectively, [2 mg/mL], which were all loaded with DiL. Here, cells treated with blank NPs without DiL loading were set as control. After incubating for different time periods [1, 3, and 5 h], the cells were rinsed with cooled PBS three times. Then, the treated cells were harvested for flow cytometry analysis.

2.8. Folate receptor expression evaluation

For western blot [WB], Cells were lysed in radioimmune precipitation assay buffer [150 mM NaCl, 0.5% sodium deoxycholate, 50 mM Tris-HCl, pH 8, sodium dodecyl sulphate [SDS] 0.1%, 0.1% Nonidet P-40] supplemented with protease inhibitors [Roche Diagnostics] for 30 min on ice. Homogenates were centrifuged at 16 000 g for 20 min at 4°C. Total cell lysates were resolved on polyacrylamide gels and transferred to nitrocellulose membranes [Bio-Rad]. Membranes were then probed with relevant primary antibodies: anti-folate-receptor [FR] [dilution 1:1000] and anti-β-actin [dilution 1:5000]. After washing, membranes were incubated with appropriate horseradish peroxidase-conjugated secondary antibodies [dilution 1:5000, GE Healthcare Biosciences, Pittsburgh, PA, USA], and blots were detected using the Enhanced Chemiluminescence Detection kit.

For immunofluorescence detection, colon-26 cells and activated Raw 264.7 macrophage cells with the concentration of 1×10^5/well were seeded in eight-chamber tissue culture glass slides [Tissue-Tek; Sakura, USA] overnight. Then cells were washed briefly with PBS and fixed by cold acetone for 2 min. After blocking, the cells were incubated with rabbit anti-FR [4 μg/mL] and with anti-rabbit conjugated with Alexa 488 secondary antibody [4 μg/mL]. Cells were coverslip-mounted with mounting medium containing 4-, 6-diamidino-2-phenylindole [DAPI]. Observations and acquisition were performed with fluorescence microscopy.

2.9. Animals

FVB/NJ mice [6–8 weeks old] were purchased from Jackson Laboratories [Bar Harbor, ME, USA]. Mice were housed under specific pathogen-free conditions. All the experiments involving mice were approved by the Institutional Animal Care and Use Committee [IACUC] of Georgia State University [Atlanta, GA, USA].

2.10. Ulcerative colitis and UC wound-healing models

For the UC model, FVB/NJ mice were induced by adding 2.5% [w/v] dextran sodium sulphate [DSS] 36–50 kDa [MP Biomedicals; Santa Ana, CA, USA] in drinking water for 7 days. In experiment groups, mice were also orally administered NPs-PEG-FA/6-shogaol [equal to 15 mg/kg 6-shogaol] in hydrogel, which comprised chitosan and alginate,[32–35] and 6-shogaol [15 mg/kg] every day. The DSS solution was freshly prepared every other day. Body weight, faeces, and physical activity were monitored daily. After 7 days, mice were killed by CO_2 euthanasia, spleens were taken out and weighed, and small pieces of distal colon were collected for RNA analysis and histopathological analysis.

For the UC wound-healing model, mice were orally administrated 2.5% [w/v] dextran sodium sulphate [DSS] 36–50 kDa [MP Biomedicals; Santa Ana; CA, USA] in drinking water for 7 days, then were treated with NPs-PEG-FA/6-shogaol [equal to 15 mg/kg 6-shogaol] in hydrogel and 6-shogaol [15 mg/kg] for 7 days. the DSS-group mice were only changed to regular water and without any treatment. Finally, mice were killed by CO_2 euthanasia and distal colons were collected for RNA analysis and histopathological analysis.

The choice of 6-shogaol [15 mg/kg] dosage is based on the human PK studies performed in the previous study,[36,37] where free forms of ginger compounds including 6-shogaol were detected in the human blood plasma upon oral administration of 2 g ginger extract [GE]. Upon normalising for a 75 kg body weight, this 2 g GE is equivalent to 25 mg/kg. Given the faster metabolic rate in mice compared with humans and the allometric scaling factor of 10,[38] and the 6-shogaol abundance in GE,[39] we chose the dosage of 15 mg/kg for *in vivo* study.

2.11. Cellular internalisation of NPs-PEG-FA *in vivo*

To track NPs-PEG-FA in gastrointestinal [GI] tract after oral administration, near infrared dye, DiR, was employed as a fluorescence

probe. Colitis was induced in FVB female mice by 2.5% [w/v] in water for 7 days. NPs-PEG-FA/DiR or NPs-PEG/DiR-embedded hydrogel was orally administered. After 6 and 12 h administration, GI tracts of mice were collected, and images were captured using IVIS *in vivo* imaging system [Perkin Elmer; Waltham, MA, USA].

2.12. Quantification of lipocalin-2

To quantify lipocalin-2 [Lcn-2], freshly collected mouse faeces were reconstituted in PBS containing 0.1% Tween 20 [50 mg/mL] and vortexed for 20 min to yield a homogeneous faecal suspension. Samples were then micro-centrifuged for 10 min at 4°C at full speed, and supernatants were collected for analysis [1: 20 dilution]. Levels of Lcn-2 were estimated using a Duoset mouse Lcn-2 ELISA kit [RandD Systems].

2.13. Monitoring of inflammation *in vivo*

Bioluminescence imaging was done using IVIS series preclinical *in vivo* imaging systems. Images of mice per group were captured and analysed with Living Image® software [Perkin Elmer; Waltham, MA, USA]. The inflammation of the gastrointestinal tract was assessed with the bioluminescent XenoLight RediJect Inflammation Probe, which is offered in a ready-to use format and can be conveniently applied to study myeloperoxidase [MPO] activity of activated phagocytes. The abdominal region was softly shaved to reduce the absorption of light. Inflammation probe [150 µl/mouse, 40 mg/mL] was injected intraperitoneally [i.p.] 5 min before imaging. The IVIS settings were epi-bioluminescence [EPI-BLI], Em-filter open, Ex-filter block, f stop 1, binning 8, exposure 300 s and focus C [6.5 cm]. Bioluminescence signals in regions of interest [ROI] were used for statistical analysis of treatment effects.

2.14. Real-time polymerase chain reaction

Total RNA was extracted from colon tissues using an RNeasy mini Kit [Qiagen; Valencia, CA, USA] according to the manufacturer's instructions. Yield and quality of extracted RNA were verified with a Synergy 2 plate reader [BioTek; Winooski, VT, USA]. cDNA was generated from the total RNA isolated above using a Maxima First-Strand cDNA Synthesis kit [Thermo Scientific; Lafayette, CO, USA]. Expression of target mRNAs was quantified by real-time reverse transcription-polymerase chain reaction [qRT-PCR] using Maxima SYBR green/ROX [6-carboxyl-X-rhodamine] qPCR Master Mix, and primer pairs are showed in Supplementary Table 1, available as Supplementary data at *ECCO-JCC* online.

2.15. Statistical analyses

One-way and two-way analyses of variance [ANOVA] and *t*-tests were used to determine statistical significance [$*p < 0.05$, $**p < 0.01$, $***p < 0.001$].

3. Results

3.1. Preparation and characterisation of NPs-PEG-FA

We prepared NPs-PEG-FA using a versatile single-step surface-functionalising technique [Figure 1A]. PLA-PEG-FA block copolymer was added to a PLGA polymer/6-shogaol emulsion; due to the differential behaviour of the hydrophobic and hydrophilic segments of PLA-PEG-FA block copolymer at the oil/water interface, PLA-PEG-FA spontaneously localised to and oriented at the surfaces of the PLGA NPs. We then removed the organic solvent by evaporation to obtain NPs-PEG-FA. As shown in representative TEM images, NPs-PEG [Figure 1B] and NPs-PEG-FA [Figure 1C] were spherical in shape and exhibited narrow size distributions. We also used dynamic light scattering [DLS] to measure their particle sizes and zeta potentials. The average hydrodynamic diameters of NPs-PEG and NPs-PEG-FA were about 246.4 ± 0.8 nm and 249.6 ± 1.3 nm, respectively, and their zeta potentials were -29.37 ± 1.58 mV and -24.17 ± 0.41 mV, respectively. These data indicate that the morphology, size distribution, and zeta potential of the NPs were not significantly changed by the addition of the folate-conjugated copolymer.

We then encapsulated 6-shogaol in the NPs. HPLC revealed that the drug loading and encapsulation efficiencies of 6-shogaol in NPs-PEG-FA were 35.8 ± 7.2 µg/mg and 52 ± 3.4%, respectively [Supplementary Figure 1, available as Supplementary data at *ECCO-JCC* online]. We investigated the release profiles of 6-shogaol from the NPs *in vitro*. As shown in Supplementary Figure 2 [available as Supplementary data at *ECCO-JCC* online], NPs-PEG and NPs-PEG-FA showed similar drug release profiles, with about 40% of the encapsulated 6-shogaol undergoing release from the NPs within the first 24 h. Both NPs-PEG and NPs-PEG-FA nanoparticles achieved cumulative 6-shogaol releases of about 80% over 72 h. These results indicate that 6-shogaol can migrate from the hydrophobic core of PLGA to the NP surface, to yield a sustained release profile and achieve controlled drug release.

3.2 Biocompatibility of NPs-PEG-FA *in vitro* and *in vivo*

For a potential DDS, biocompatibility is a key issue that should be carefully considered. To analyse potential cytotoxicity, we first investigated the effects of NPs, NPs-PEG, and NPs-PEG-FA on colon-26 cells and Raw 264.7 macrophage cells *in vitro* using the MTT cell proliferation assay. We found that treatment with each nanoparticle for 24 h did not alter the viability of colon-26 cells [Supplementary Figure 3A, available as Supplementary data at *ECCO-JCC* online] or Raw 264.7 cells [Supplementary Figure 3C] at any tested concentration [up to 1 mg/mL]. When we extended the incubation time to 48 h, the cell viability of colon-26 cells was unchanged [Supplementary Figure 3B]. At 48 h, the cell viability of Raw 264.7 macrophage cells was dramatically decreased in the NP-treated group, but not in the NPs-PEG- or NPs-PEG-FA-treated groups [Supplementary Figure 3D]. This indicates that PEG modification increased the biocompatibility of the studied NPs.

To investigate the toxicity of NPs-PEG-FA *in vivo*, healthy mice were orally administered NPs-PEG-FA or PBS [control] for 7 days. At the end of the experiment [7 days treatment], body weight changes were compared, bloods were collected for haematological and biochemical analyses, and tissues from the gastrointestinal [GI] tract and major organs [heart, liver, spleen, lung, and kidney] were collected for histological analysis. There was no remarkable difference in the body weight change, haematological parameters, or biochemical findings of the NPs-PEG-FA-treated mice compared with controls [Figure 2A–C]. We also failed to find any notable sign of toxicity in tissues from the GI tract [Figure 2D] or heart, liver, spleen, lung, or kidney [Supplementary Figure 4, available as Supplementary data at *ECCO-JCC* online]. These data indicate that NPs-PEG-FA do not appear to have any obvious toxicity *in vivo*. Taken together, our findings indicate that NPs-PEG-FA exhibit excellent biocompatibility *in vitro* and *in vivo*, and thus could be safely used as a drug delivery vehicle.

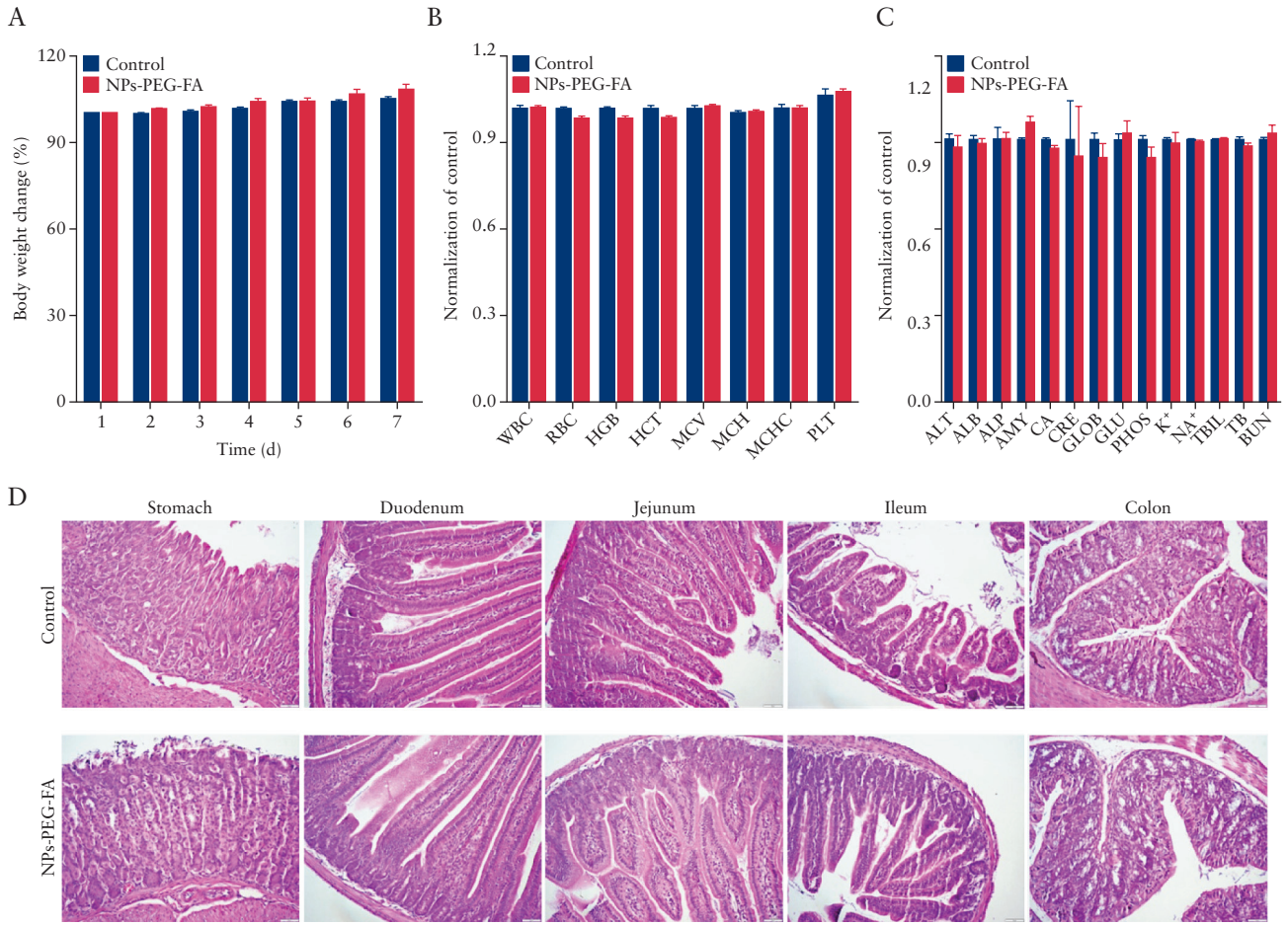

Figure 2. NPs-PEG-FA is biocompatible. To evaluate the biocompatibility of NPs-PEG-FA *in vivo*, mice were orally administered wNPs-PEG-FA [15 mg in PBS] or phosphate-buffered solution [PBS] [control] for 7 days. Experiments were performed on five mice per group [n = 5] throughout. A: Body weight change. Body weights were measured in each group and normalised by the corresponding initial body weight. B: Blood was collected by intracardiac puncture with a syringe, and haematological analyses were performed using an automatic haematology analyser [VetScan HM5; Abaxis, CA, USA]. The following haematologic parameters are shown: WBC, total white blood cells; LYM, lymphocytes; MON, monocytes; NEU, neutrophils; RBC, red blood cells; HGB, haemoglobin; PLT, platelets; ALT, alanine aminotransferase; and AST, aspartate aminotransferase. C: Blood was collected and biochemical analyses were performed using a biochemical analyser [VetScan VS2; Abaxis, CA, USA] with a comprehensive diagnostic profile reagent rotor. The following biochemical parameters were assessed: ALT, alanine aminotransferase; ALB, albumin; ALP, alkaline phosphatase; AMY, amylase; CA, calcium; CRE, creatinine; GLOB, globulin; GLU, glucose; PHOS, phosphorus; TBIL, total bilirubin; TP, total protein; and BUN, urea nitrogen. D: haematoxylin and eosin [H & E] staining of histological sections was used to assess the toxicity of NPs-PEG-FA toward gastro-intestinal tissues [stomach, duodenum, jejunum, ileum, and colon].

3.3 NPs-PEG-FA are taken up by macrophages and epithelial cells

Efficient cellular uptake of NPs is a major requirement for their therapeutic efficacy. Folate has been shown to increase the cellular uptake of nanocarrier systems by targeting the folate receptor.[40–43] To confirm the activity of the folate molecules on the surfaces of NPs-PEG-FA, we performed *in vitro* cell uptake studies using fluorescently [DiL]-labelled NPs in colon-26 epithelial-like and activated Raw 264.7 macrophage-like cells. The expressions of folate receptor on these two cell lines were confirmed by western blotting [Supplementary Figure 5A, available as Supplementary data at *ECCO-JCC* online] and immunofluorescence staining [Supplementary Figure 5B]. We incubated NPs-PEG and NPs-PEG-FA with colon-26 cells and activated Raw 264.7 cells at 37°C for 6 h. Subsequent fluorescence microscopy revealed that cells incubated with NPs-PEG-FA showed strong NP-associated [DiL, red] fluorescence inside the cells but only a few red dots on the membrane [Figure 3A, b and d]. In contrast, no fluorescence was observed inside or at the surface of NPs-PEG-treated cells [Figure 3A, a and c]. These results suggest that folate receptor could be involved in the uptake of folate-functionalised NPs but not in that of non-targeted NPs. Cellular uptake was also assessed by flow cytometry, which revealed much stronger fluorescence in colon-26 cells [Figure 3B] and activated Raw 264.7 cells [Figure 3C] treated with NPs-PEG-FA versus NPs-PEG. These results are consistent with the idea that NPs-PEG-FA undergoes folate-receptor-mediated endocytosis.

We further used flow cytometry to compare the cellular uptake efficiencies of NPs-PEG-FA with three different amounts of surface-displayed FA. Here, NPs-PEG-FA-1, 2, and 3 were defined as 10%, 15%, and 20% [w/w] of PLA-PEG-FA in total polymers. As shown in Figure 4, the various NPs were incubated with colon-26 cells and activated Raw 264.7 cells for 1, 3, and 6 h. NPs-PEG-FA-1 exhibited a higher internalisation efficiency in colon-26 cells, whereas NPs-PEG-FA-1, -2, and -3 had similar internalisation efficiencies in activated Raw 264.7 cells. These results indicated that surface functionalisation with FA enabled the NPs to experience an enhanced

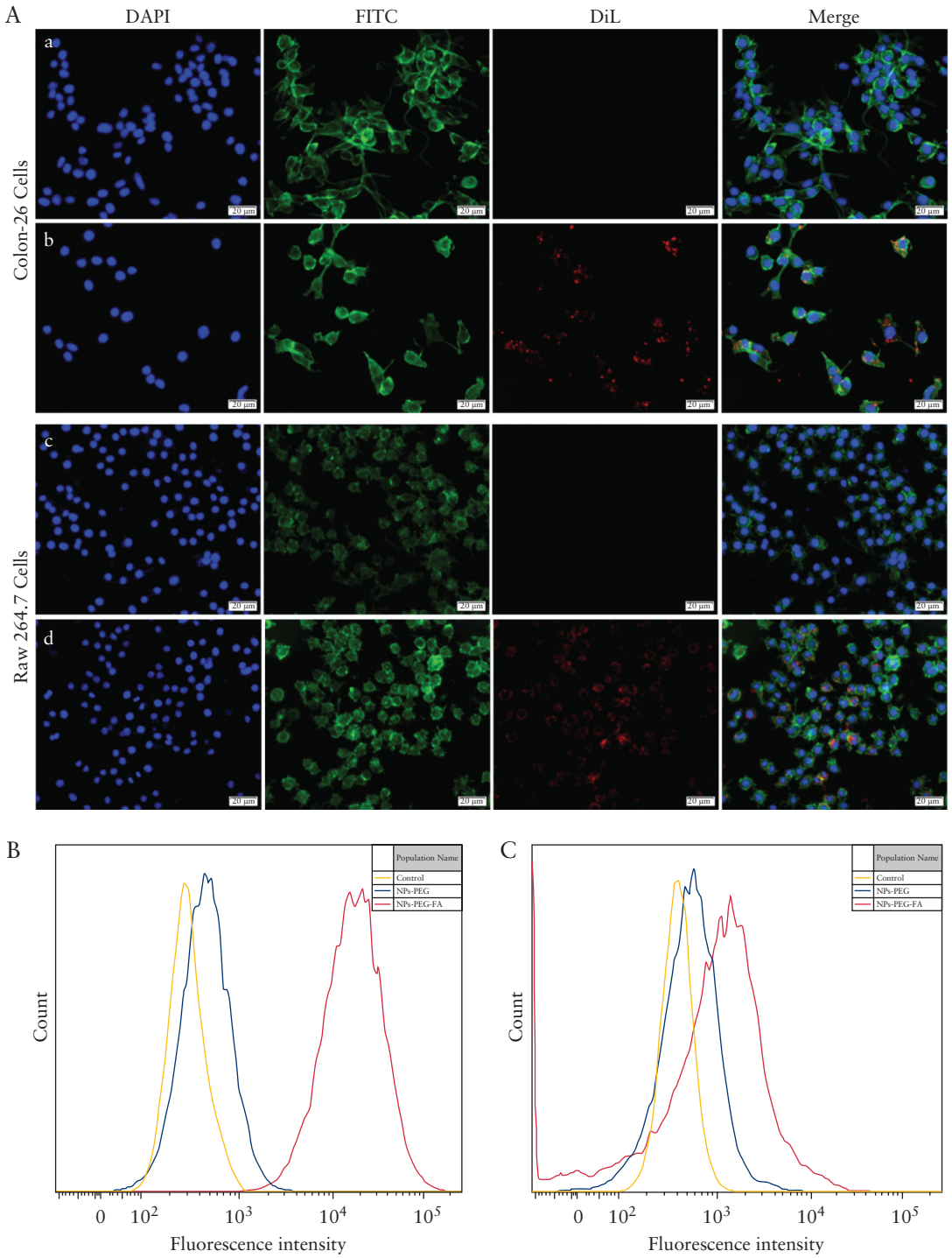

Figure 3. NPs-PEG-FA are taken up by macrophages and epithelial cells through folate receptor-mediated endocytosis. A: Colon-26 cells and activated Raw 264.7 cells were incubated with NPs-PEG/DiL or NP-PEG-FA/DiL for 6 h. Here, DiL was a fluorescent dye and used as a tracker. The colours are as follows: blue channel, DAPI; green channel, FITC; and red channel, DiL. Panels: a, colon-26 cells incubated with NPs-PEG/DiL; b, colon-26 cells incubated with NPs-PEG-FA/DiL; c, activated Raw 264.7 cells incubated with NPs-PEG/DiL; and d, activated Raw 264.7 cells incubated with NPs-PEG-FA/DiL. B and C: Flow cytometry was used to quantify the fluorescence intensity of DiL in colon-26 cells [B] and activated Raw 264.7 cells [C] treated as described above and incubated for 6 h. In all experiments, $n = 5$; the scale bar in [A] = 20 μm.

cellular uptake that was directly related to the amount of surface-functionalised FA. These data are consistent with previous reports.[42] Based on our findings, we used NPs-PEG-FA-1 for the following experiments.

3.4 The uptake of NPs-PEG-FA by the intestinal mucosa is increased during colitis

The accumulation of NPs in the colon region is one the most important features of an effective nanomedicine for colon diseases, such as

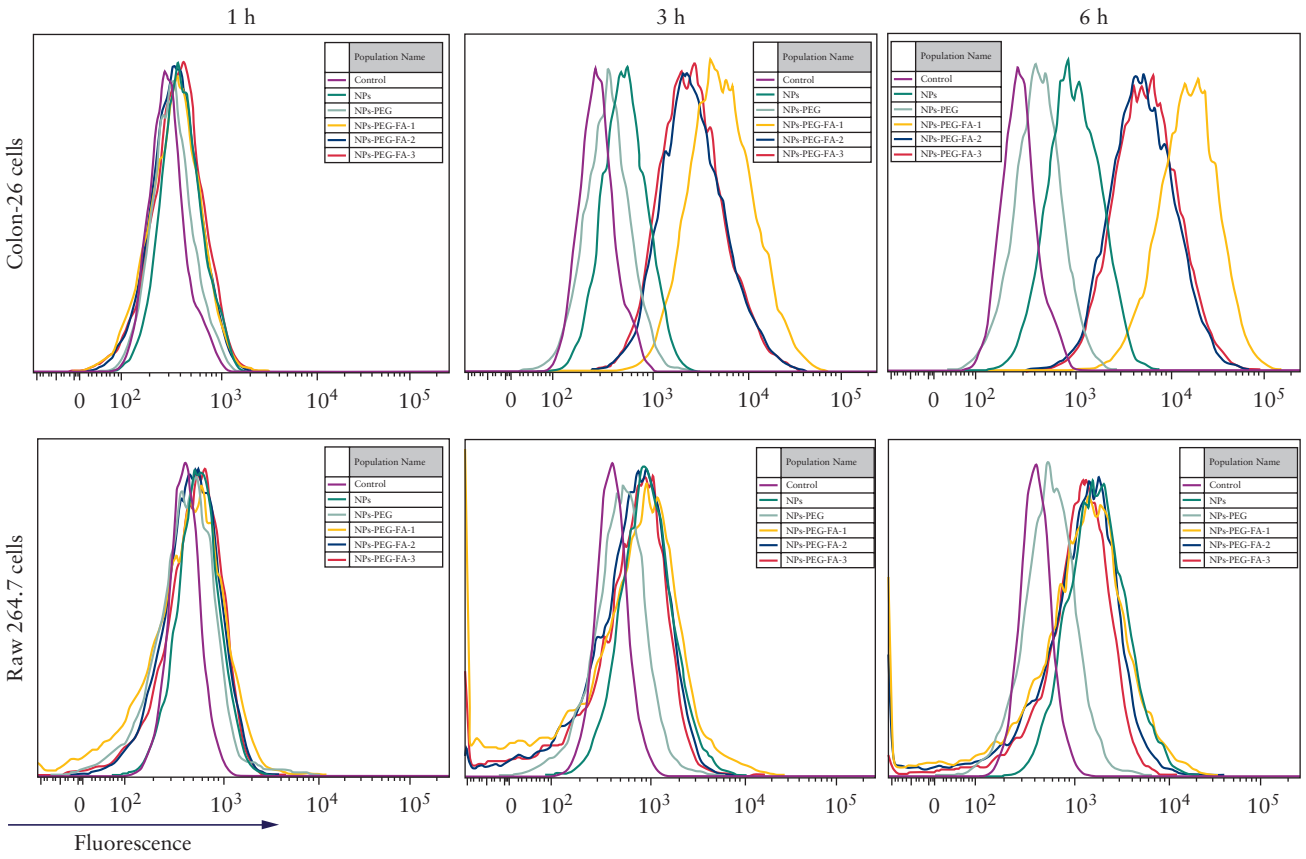

Figure 4. Folate mediates the uptake of NPs-PEG-FA by macrophages and epithelial cells. Colon-26 cells and activated Raw 264.7 cells were incubated with NPs, NPs-PEG, NPs-PEG-FA-1, NPs-PEG-FA-2, or NPs-PEG-FA-3. NPs-PEG-FA-1, 2, and 3 were defined as 10%, 15%, and 20% [w/w] of PLA-PEG-FA in total polymers. After 1, 3, or 5 h of incubation, the cells were rinsed three times with cool phosphate-buffered saline [PBS] and harvested for flow cytometry analysis; uptake efficiency was evaluated according to the fluorescence intensity [n = 5].

ulcerative colitis [UC]. To achieve such accumulation, we encapsulated NPs-PEG-FA in a hydrogel system comprising alginate/chitosan with a special weight ratio [3/7]. Our previous research showed that this hydrogel system can deliver and release encapsulated nanoparticles to the colon region in response to the specific pH found in the colon.[32–35] To investigate the *in vivo* biodistribution of NPs-PEG-FA in the GI tract, we orally dosed DSS-treated colitic mice with DiR-loaded NPs-PEG-FA in our hydrogel system, and used an *in vivo* imaging system [IVIS] to examine the near-infrared fluorescence of DiR in the GI tract at 6 h and 12 h post-administration [Figure 5A]. We found that colitic mice treated with NPs-PEG-FA/DiR exhibited significantly stronger DiR fluorescence intensity in the colon compared with NPs-PEG/DiR-treated mice, at both 6 h and 12 h post-administration [Figure 5B]. Fluorescence imaging of colitis tissues also confirmed that oral administration of NPs-PEG-FA in the hydrogel system resulted in the delivery of NPs-PEG-FA to the colon and their uptake by colonic cells [Figure 5C]. The expression of folate receptor was enhanced in colitis tissues [Supplementary Figure 6, available as Supplementary data at *ECCO-JCC* online], allowing us to conclude that the enhanced colitis tissue uptake of NPs-PEG-FA appears to reflect receptor-mediated endocytosis.

3.5 Oral administration of NPs-PEG-FA/6-shogaol attenuates UC

Having confirmed that NPs-PEG-FA in our hydrogel system can preferentially target the colon, we next assessed whether NPs-PEG-FA/6-shogaol can attenuate DSS-induced UC, which is a well-established mouse model for studying human UC.[44,45] Mice were provided with DSS-laced water for 7 days with or without simultaneous daily oral administration of NPs-PEG-FA/6-shogaol or 6-shogaol. To assess the progression of intestinal inflammation, we used ELISA to assess the faecal levels of lipocalin-2 [Lcn-2], which is a widely accepted biomarker for intestinal inflammation.[46] As shown in Figure 6A, the basal levels of Lcn-2 in the different treatment groups were similarly low on Day 1 to Day 3. In the DSS and DSS plus 6-shogoal groups, the Lcn-2 level dramatically increased beginning on Day 5. By comparison, the Lcn-2 level in the DSS plus NPs-PEG-FA/6-shogaol group was significantly lower than the levels in the DSS control and DSS plus 6-shogoal groups on Day 5 and thereafter. These results suggest that NPs-PEG-FA/6-shogaol exerts excellent anti-inflammatory effects and appears to attenuate DSS-induced UC.

To further assess treatment effects at a quantitative level, we employed *in vivo* bioluminescence imaging using the inflammation probe [XenoLight™; MA, USA],[47,48] which allowed us to longitudinally track the myeloperoxidase [MPO] level and inflammation status *in vivo*. As shown in Figure 6B and C, DSS treatment was associated with an increased bioluminescence signal that reflected severe intradigestive inflammation. However, and consistent with our Lcn-2 data, this bioluminescence signal was significantly lower in DSS plus NPs-PEG-FA/6-shogaol-treated mice versus the DSS control group.

At the end of the experiment, mice were sacrificed. We found that those treated with NPs-PEG-FA/6-shogaol exhibited

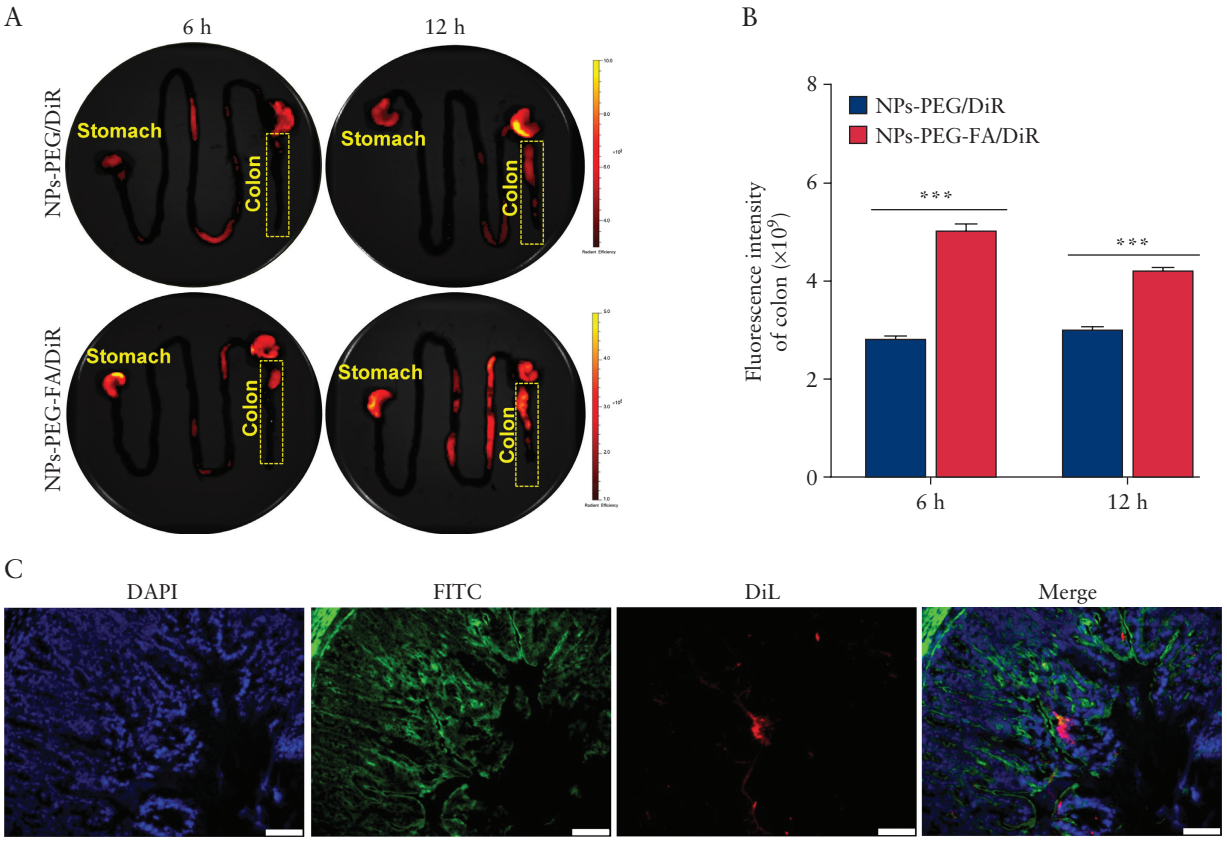

Figure 5. NPs-PEG-FA uptake is increased during colitis in mice. A: DiR-loaded NPs-PEG and NPs-PEG-FA were orally administered to colitic mice, and images were obtained at 6 h and 12 h post-administration using an *in vivo* imaging system [IVIS]. B: Fluorescence intensities were quantified and compared in the colon at 6 h and 12 h post-dosing [$n = 3$]. C: Colitis tissue uptake of orally administered NPs-PEG-FA in hydrogel at 12 h post-dosing. Fixed colitis tissues were stained with FITC-phalloidin [green channel] and DAPI [blue channel] for visualisation of actin and nuclei, respectively. Scale bar = 50 μm.

significantly decreased spleen/body weight [Figure 6D], indicating reduced inflammation with NPs-PEG-FA/6-shogaol treatment. The histological effects of NPs-PEG-FA/6-shogaol on DSS-induced UC were examined by haematoxylin and eosin [H&E] staining. Mice treated with DSS alone exhibited robust signs of inflammation, including epithelial erosion, interstitial oedema, and a general increase in the number of inflammatory cells in the lamina propria [Figure 6E, b, arrowhead]. In contrast, mice treated with DSS plus NPs-PEG-FA/6-shogaol showed decreases in these signs of UC at the histological level, including a particularly notable decrease of local lymphocytic infiltration [Figure 6E, d].

We also determined the mRNA expression levels of pro- and anti-inflammatory genes in the different treatment groups. As shown in Figure 6F, the expression levels of the pro-inflammatory genes, TNF-α, IL-6, IL-1β, and iNOS, were increased significantly in DSS-treated mice, whereas these increases were significantly ameliorated in the DSS plus NPs-PEG-FA/6-shogaol group. Treatment with NPs-PEG-FA/6-shogaol was also associated with increase in the anti-inflammatory genes, nuclear factor [erythroid-derived 2]-like 2 [Nrf-2], and haeme oxygenase [HO-1]. These findings indicate that NPs-PEG-FA/6-shogaol confers anti-inflammatory effects against DSS-induced colitis by blocking the production of damaging pro-inflammatory genes while enhancing the production of anti-inflammatory genes.

3.6 Oral administration of NPs-PEG-FA/6-shogaol accelerates colitis wound repair

The ability of modulatory factors to enhance intestinal repair mechanisms may form the basis of future approaches for treating diseases characterised by injury to the epithelial surface.[49] Based on our finding that simultaneously administered NPs-PEG-FA/6-shogaol could attenuate DSS-induced UC, we next tested whether NPs-PEG-FA/6-shogaol could help heal the inflamed mucosa when applied subsequent to the administration of DSS. As shown in Figure 7A, colitis was induced by DSS from Day 1-Day 7 [colitis phase], and recovery was from Day 7-Day 13 [recovery phase] induced by plain water, NPs-PEG-FA/6-shogaol, and free 6-shogaol, respectively. The Lcn-2 levels of mice treated with DSS alone gradually increased from Day 1 to Day 7 and thereafter remained high, indicating active intestinal inflammation. In contrast, mice treated with DSS followed by NPs-PEG-FA/6-shogaol had lower Lcn-2 levels than the DSS group from Day 7-Day 13 and had almost completely recovered their pretreatment Lcn-2 levels at Day 13. This was further confirmed by *in vivo* bioluminescence imaging using an inflammation probe [XenoLight™; MA, USA]. As shown in Figure 7B, mice of the NPs-PEG-FA/6-shogaol group displayed significantly lower luminescence intensity on Day 13, at a level that indicated the presence of only negligible inflammation in the GI tract. Similarly, histological analysis confirmed that the ulceration of the intestinal mucosa and the extent of neutrophil infiltration were

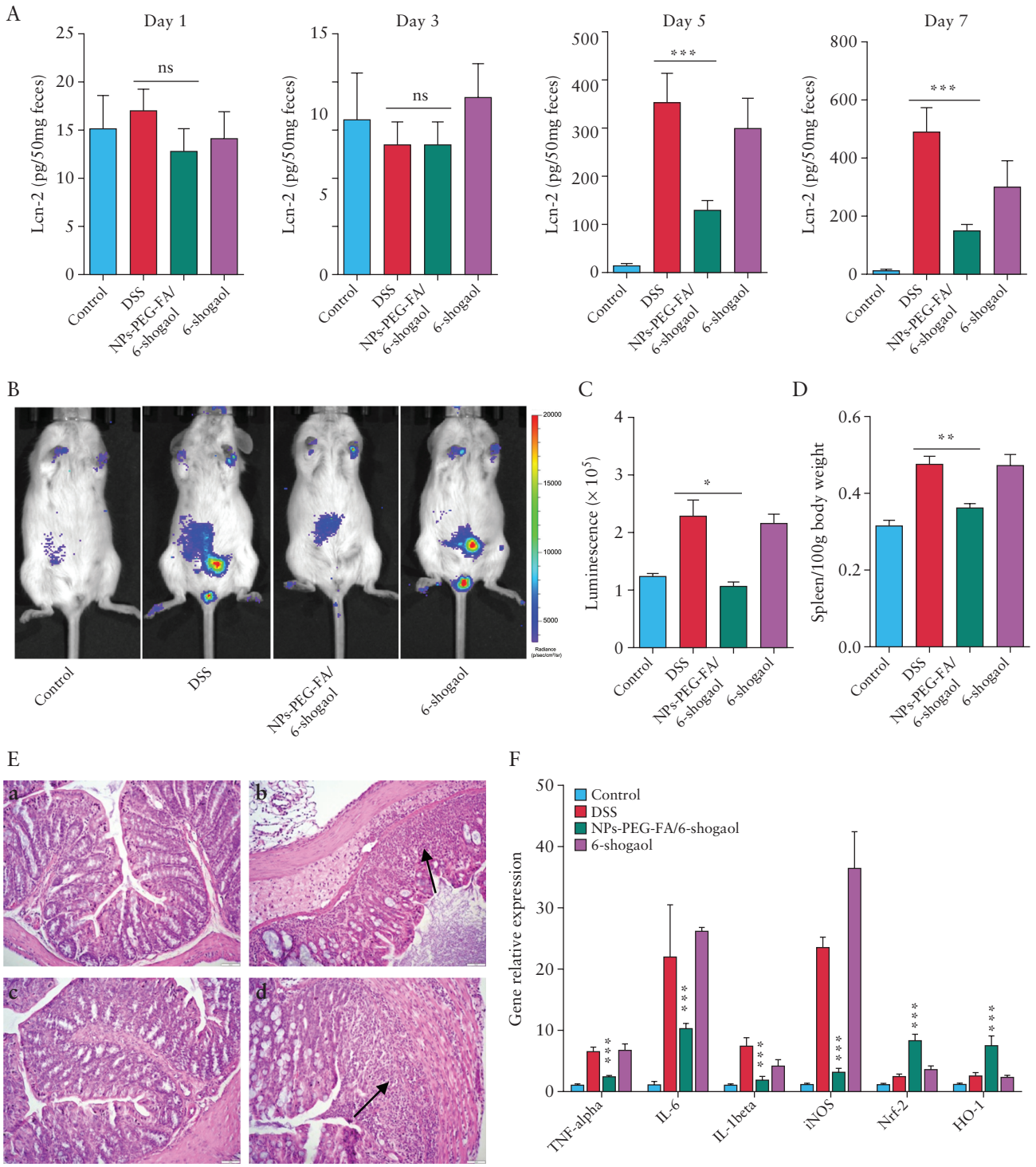

Figure 6. Protective effect of NPs-PEG-FA/6-shogaol on dexrtran sodium sulphate [DSS]-induced colitis. A: enzyme-linked immunosorbent assay [ELISA] was used to quantify faecal lipocalin-2 [Lcn-2] levels in mice on Days 1, 3, 5, and 7 of DSS treatment with or without co-administration of NPs-PEG-FA/6-shogaol. B: Bioluminescence images of mice treated with an inflammation probe [XenoLight™; MA, USA], as captured by IVIS. Mice were intraperitoneally [i.p.] injected with inflammation probe [200 mg/kg; 150 µL/mouse]. At 5 min post-injection, images were obtained using a 5-min exposure time [for improved sensitivity]. C: The bioluminescence intensities of mice were quantified and compared between groups [n = 5]. D: At the end of the experiment, mice were sacrificed and the spleen/body weight of each group was compared [$n = 5$]. E: Colon histology was examined by haematoxylin and eosin [H & E] staining. At the end of experiment, colons were collected from the different treatment groups, 6-µm thick tissue sections were prepared, H & E staining was applied, and histological assessment was performed. Inflammatory cells in the lamina propria are indicated by arrowheads. Representative sections are shown [$n = 5$/group]. Scale = 20 µm. Panels: a, control mice; b, DSS-treated mice; c, DSS plus NPs-PEG-FA/6-shogaol treated mice; and d: DSS plus free 6-shogaol-treated mice. F: The mRNA expressions of various genes were quantified by real-time polymerase chain reaction [PCR] [$n = 5$]; ***$p < 0.001$.

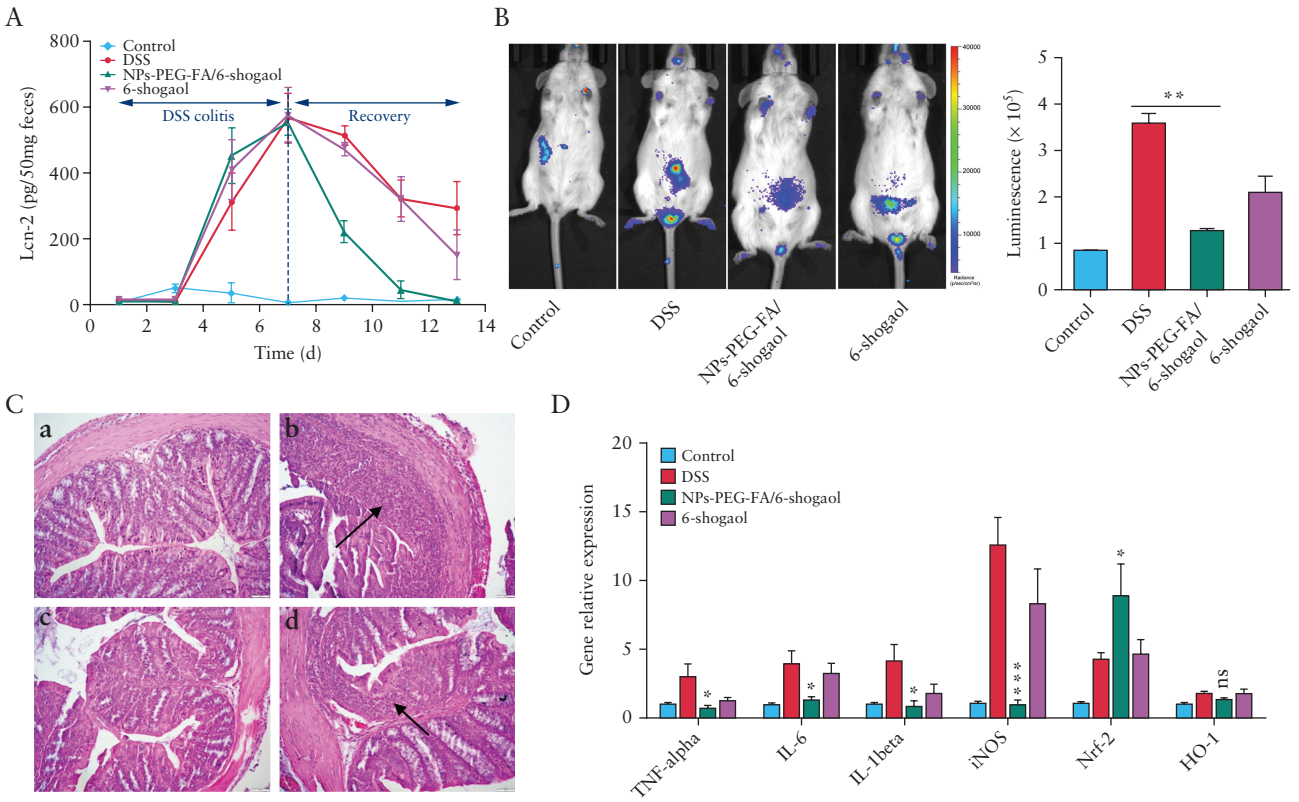

Figure 7. Therapeutic effect of NPs-PEG-FA/6-shogaol on DSS-induced colitis. A: enzyme-linked immunosorbent assay [ELISA] was used to quantify faecal Lcn-2. During the dextran sodium sulphate [DSS] colitis phase, mice of all groups were given DSS water. During the recovery phase, mice were given plain water and the appropriate groups were orally treated with NPs-PEG-FA/6-shogaol or free 6-shogaol for 7 days [$n = 5$]. B: Bioluminescence images of mice were obtained using the inflammation probe and IVIS, and intensities were compared [$n = 5$]. C: Haematoxylin and eosin [H & E] staining was used for histological assessment. Inflammatory cells in the lamina propria are indicated by arrowheads [$n = 5$]. Panels: a, control mice; b, DSS-treated mice; c, DSS plus NPs-PEG-FA/6-shogaol-treated mice; and d, DSS plus free 6-shogaol-treated mice. D: The mRNA expressions of various genes were quantified by real-time polymerase chain reaction [PCR] [$n = 5$]. Symbols: $^*p < 0.05$; $^{***}p < 0.001$; and ns, no significant difference.

lower in NPs-PEG-FA/6-shogaol-treated mice [Figure 7C]. Finally, in NPs-PEG-FA/6-shogaol-treated mice, the mRNA expression levels of certain pro-inflammatory cytokines [TNF-α, IL-6, IL-1β] and iNOS were significantly decreased at the end of the recovery phase, whereas that of Nrf-2 [no significant difference of HO-1] was enhanced [Figure 7D] relative to the control group, suggesting that oral administration of NPs-PEG-FA/6-shogaol could accelerate colitis wound repair by regulating gene expression.

4. Discussion

The development of colon-targeted oral delivery systems represents an active area of research for treating diseases that affect the colon, particularly ulcerative colitis [UC]. The existing strategies for colon-targeted delivery include pH-dependent, time-dependent, and microflora-enzyme dependent systems. Although pH-dependent systems may survive passage through the stomach,[50] time-dependent systems usually depend on the typical duration it takes food and drugs to passage through the GI tract, which can be irregular especially in disease states.[51] Recently, nanotechnology has emerged as a novel and efficient tool for targeted drug delivery. Upon oral administration, nanoparticle-based drug delivery systems [DDSs] may protect a loaded drug from the harsh gastrointestinal environment and selectively increase the concentration of the drug at the disease site.

Among the developed NPs, polymeric NPs, especially those formulated using lactide:glycolide [PLGA] copolymer, have emerged as promising carriers for the targeted colonic delivery of various payloads, including drugs, siRNAs, and proteins. PLGA NPs have the advantages of biodegradability, biocompatibility, ease of formulation, and tunable sustained drug release properties.[52,53] However, a striking drawback for PLGA NPs is the limited number of surface-displayed functional groups that may be employed for targeting ligands.[54,55] In the present work, we took full advantage of the differential behaviour of the hydrophobic and hydrophilic segments of PLA-PEG-FA block copolymers at the oil/water interface. This enabled folate-functionalised PLGA/PLA-PEG-FA NPs to be easily fabricated using a versatile single-step surface-functionalising technique. Critically, our PEG-chain-modified NPs exhibited excellent biocompatibility *in vitro* and *in vivo*, indicating they can be used as a safe drug delivery carrier.

Ginger, which shows anti-inflammatory and anti-oxidative properties, has long been used in traditional medicine to treat numerous ailments, including digestive issues [indigestion, constipation, and ulcers] and degenerative disorders [arthritis and rheumatism].[56,57] A major component of dried ginger, 6-shogaol, has been a prime focus of the *in vitro* research related to the anti-inflammatory effects of ginger. However, there has not been any systematic study of the *in vivo* anti-inflammatory effects of 6-shogaol, especially in the context of inflammatory bowel diseases [IBDs]. In the present work, we show that 6-shogaol loaded in a colon-targeting delivery carrier appears to significantly alleviate colitis symptoms and accelerate colitis wound repair in the DSS-induced mouse model of colitis.

Mechanistically, our real-time PCR results indicate that 6-shogaol exerts its anti-inflammatory effects by regulating several important molecular targets. It suppresses several pro-inflammatory cytokines [TNF-α, IL-6, and IL-1β] that are characteristically upregulated in DSS-induced colitis,[58] as well as inducible nitric oxide synthase [iNOS], which produces nitric oxide [NO] and is involved in the pathogenesis of colitis.[59] Conversely, 6-shogaol promotes the expression of nuclear factor [erythroid-derived 2]-like 2 [Nrf-2] and haeme oxygenase 1 [HO-1], which play important roles in anti-inflammation and anti-oxidation.[60–62] The potential anti-inflammatory mechanisms of 6-shoagol in IBD have not been systematically demonstrated yet. However, the clear mechanisms of 6-shogaol in other systems could benefit us as background. For example, Chen *et al.* identified Nrf-2 as a molecular target of 6-shogaol in colon epithelial cells both *in vitro* and *in vivo*, and they demonstrated that 6-shogaol induced nuclear translocation of Nrf-2 and activated Nrf-2 target genes in an Nrf-2-dependent manner.[61] Mitogen-activated protein kinases [MAPKs] have been associated with the Nrf-2 pathway in an inducer- and cell type-dependent manner.[63] PI3K have also been extensively investigated for its regulation of Nrf-2.[64,65] These findings suggest that MAPKs and the PI3K/AKT pathway participate in 6-shogaol induced Nrf-2 activation in HCT-116 cells. Luettig *et al.* confirmed that 6-shogaol has barrier-protective effects by affecting TNF-α induced claudin-2 upregulation and claudin-1 disassembly via inhibition of PI3K/AKT and NF-κB light chain enhancer of activated B-cell signalling, suggesting 6-shogaol might be beneficial for barrier preservation during intestinal inflammation.[58] In addition, the proposed mechanism behind 6-shogaol inhibition of NO evolution in stimulated macrophages involves downregulation of inflammatory iNOS and COX-2 gene expression by inhibition of the activation of NF-κB, because NF-κB plays a critical role in the coordination of the expressions of pro-inflammatory enzymes[66]; inhibition of DNA-binding activity of NF-κB corresponds to the expressional inhibition of iNOS, COX-2, and TNF-α.[67]

In summary, we herein used a versatile single-step surface-functionalising technique to prepare 6-shogaol-loaded PLGA/PLA-PEG-FA nanoparticles [NPs-PEG-FA/6-shogaol], and found that this NP exerts excellent biocompatibility both *in vitro* and *in vivo*. Furthermore, we show that oral administration of NPs-PEG-FA/6-shogaol in a hydrogel system could significantly alleviate colitis symptoms and accelerate colitis wound repair in DSS-induced mouse colitis. This system may represent a promising therapeutic approach for treating IBD.

Funding

This work was supported by grant from the National Institutes of Health of Diabetes and Digestive and Kidney [RO1DK071594 to DM]. MZZ was the recipient of a Research Fellowship Award from the Crohn's & Colitis Foundation. DM was a recipient of a Research Scientist Award from the Department of Veteran Affairs

Conflict of Interest

None.

Author Contributions

XCL and MZZ designed and conducted the experiments and wrote the manuscript. LXW and DDL provided technical and material support and helped with the experiments. MKH gave direct guidance for the animal experiments. DM supervised and supported this study and critically revised the manuscript.

Supplementary Data

Supplementary data are available at *ECCO-JCC* online.

References

1. de Souza HS, Fiocchi C. Immunopathogenesis of IBD: current state of the art. *Nat Rev Gastroenterol Hepatol* 2016;**13**:13–27.
2. Vavricka SR, Schoepfer A, Scharl M, Lakatos PL, Navarini A, Rogler G. Extraintestinal manifestations of inflammatory bowel disease. *Inflamm Bowel Dis* 2015;**21**:1982–92.
3. Neurath MF. Current and emerging therapeutic targets for IBD. *Nat Rev Gastroenterol Hepatol* 2017;**14**:269–78.
4. Bernstein CN. Treatment of IBD: where we are and where we are going. *Am J Gastroenterol* 2015;**110**:114–26.
5. Nielsen OH. New strategies for treatment of inflammatory bowel disease. *Front Med [Lausanne]* 2014;**1**:3.
6. Hua S, Marks E, Schneider JJ, Keely S. Advances in oral nano-delivery systems for colon targeted drug delivery in inflammatory bowel disease: selective targeting to diseased versus healthy tissue. *Nanomedicine* 2015;**11**:1117–32.
7. Byrne CM, Solomon MJ, Young JM, Selby W, Harrison JD. Patient preferences between surgical and medical treatment in Crohn's disease. *Dis Colon Rectum* 2007;**50**:586–97.
8. Zhang S, Ermann J, Succi MD, *et al.* An inflammation-targeting hydrogel for local drug delivery in inflammatory bowel disease. *Sci Transl Med* 2015;**7**:300ra128.
9. Kriegel C, Attarwala H, Amiji M. Multi-compartmental oral delivery systems for nucleic acid therapy in the gastrointestinal tract. *Adv Drug Deliv Rev* 2013;**65**:891–901.
10. Collnot EM, Ali H, Lehr CM. Nano- and microparticulate drug carriers for targeting of the inflamed intestinal mucosa. *J Control Release* 2012;**161**:235–46.
11. Ulbrich W, Lamprecht A. Targeted drug-delivery approaches by nanoparticulate carriers in the therapy of inflammatory diseases. *J R Soc Interface* 2010;**7[Suppl 1]**:S55–66.
12. Moulari B, Pertuit D, Pellequer Y, Lamprecht A. The targeting of surface modified silica nanoparticles to inflamed tissue in experimental colitis. *Biomaterials* 2008;**29**:4554–60.
13. Pridgen EM, Alexis F, Farokhzad OC. Polymeric nanoparticle drug delivery technologies for oral delivery applications. *Expert Opin Drug Deliv* 2015;**12**:1459–73.
14. Lautenschläger C, Schmidt C, Fischer D, Stallmach A. Drug delivery strategies in the therapy of inflammatory bowel disease. *Adv Drug Deliv Rev* 2014;**71**:58–76.
15. Date AA, Hanes J, Ensign LM. Nanoparticles for oral delivery: Design, evaluation and state-of-the-art. *J Control Release* 2016;**240**:504–26.
16. Huang Z, Gan J, Jia L, *et al.* An orally administrated nucleotide-delivery vehicle targeting colonic macrophages for the treatment of inflammatory bowel disease. *Biomaterials* 2015;**48**:26–36.
17. Vafaei SY, Esmaeili M, Amini M, Atyabi F, Ostad SN, Dinarvand R. Self assembled hyaluronic acid nanoparticles as a potential carrier for targeting the inflamed intestinal mucosa. *Carbohydr Polym* 2016;**144**:371–81.
18. Xiao B, Laroui H, Viennois E, *et al.* Nanoparticles with surface antibody against CD98 and carrying CD98 small interfering RNA reduce colitis in mice. *Gastroenterology* 2014;**146**:1289–300.e1–19.
19. Xiao B, Yang Y, Viennois E, *et al.* Glycoprotein CD98 as a receptor for colitis-targeted delivery of nanoparticle. *J Mater Chem B Mater Biol Med* 2014;**2**:1499–508.
20. Chapkin RS, Kamen BA, Callaway ES, *et al.* Use of a novel genetic mouse model to investigate the role of folate in colitis-associated colon cancer. *J Nutr Biochem* 2009;**20**:649–55.
21. Spencer SP, Belkaid Y. Dietary and commensal derived nutrients: shaping mucosal and systemic immunity. *Curr Opin Immunol* 2012;**24**:379–84.
22. Zhang M, Xu C, Wen L, *et al.* A hyaluronidase-responsive nanoparticle-based drug delivery system for targeting colon cancer cells. *Cancer Res* 2016;**76**:7208–18.

23. Vimala S, Norhanom AW, Yadav M. Anti-tumour promoter activity in Malaysian ginger rhisobia used in traditional medicine. *Br J Cancer* 1999;**80**:110–6.
24. Shukla Y, Singh M. Cancer preventive properties of ginger: a brief review. *Food Chem Toxicol* 2007;**45**:683–90.
25. Chan EWC, Lim YY, Wong LF, *et al*. Antioxidant and tyrosinase inhibition properties of leaves and rhisomes of ginger species. *Food Chem* 2008;**109**:477–83.
26. Zhang M, Viennois E, Prasad M, *et al*. Edible ginger-derived nanoparticles: A novel therapeutic approach for the prevention and treatment of inflammatory bowel disease and colitis-associated cancer. *Biomaterials* 2016;**101**:321–40.
27. Zhang M, Collins JF, Merlin D. Do ginger-derived nanoparticles represent an attractive treatment strategy for inflammatory bowel diseases? *Nanomedicine [Lond]* 2016;**11**:3035–7.
28. Zhang M, Xiao B, Wang H, *et al*. Edible ginger-derived nano-lipids loaded with doxorubicin as a novel drug-delivery approach for colon cancer therapy. *Mol Ther* 2016;**24**:1783–96.
29. Zhang M, Viennois E, Xu C, Merlin D. Plant derived edible nanoparticles as a new therapeutic approach against diseases. *Tissue Barriers* 2016;**4**:e1134415.
30. Shim S, Kim S, Choi DS, Kwon YB, Kwon J. Anti-inflammatory effects of [6]-shogaol: potential roles of HDAC inhibition and HSP70 induction. *Food Chem Toxicol* 2011;**49**:2734–40.
31. Li F, Nitteranon V, Tang X, *et al*. In vitro antioxidant and anti-inflammatory activities of 1-dehydro-[6]-gingerdione, 6-shogaol, 6-dehydroshogaol and hexahydrocurcumin. *Food Chem* 2012;**135**:332–7.
32. Laroui H, Dalmasso G, Nguyen HT, Yan Y, Sitaraman SV, Merlin D. Drug-loaded nanoparticles targeted to the colon with polysaccharide hydrogel reduce colitis in a mouse model. *Gastroenterology* 2010;**138**:843–53.e1–2.
33. Laroui H, Theiss AL, Yan Y, *et al*. Functional TNFα gene silencing mediated by polyethyleneimine/TNFα siRNA nanocomplexes in inflamed colon. *Biomaterials* 2011;**32**:1218–28.
34. Xiao B, Zhang Z, Viennois E, *et al*. Combination therapy for ulcerative colitis: orally targeted nanoparticles prevent mucosal damage and relieve inflammation. *Theranostics* 2016;**6**:2250–66.
35. Xiao B, Xu Z, Viennois E, *et al*. Orally targeted delivery of tripeptide KPV via hyaluronic acid-functionalised nanoparticles efficiently alleviates ulcerative colitis. *Mol Ther* 2017;**25**:1628–40.
36. Zick SM, Djuric Z, Ruffin MT, *et al*. Pharmacokinetics of 6-gingerol, 8-gingerol, 10-gingerol, and 6-shogaol and conjugate metabolites in healthy human subjects. *Cancer Epidemiol Biomarkers Prev* 2008;**17**:1930–6.
37. Zick SM, Ruffin MT, Djuric Z, Normolle D, Brenner DE. Quantitation of 6-, 8- and 10-gingerols and 6-shogaol in human plasma by high-performance liquid chromatography with electrochemical detection. *Int J Biomed Sci* 2010;**6**:233–40.
38. Reagan-Shaw S, Nihal M, Ahmad N. Dose translation from animal to human studies revisited. *FASEB J* 2008;**22**:659–61.
39. Gundala SR, Mukkavilli R, Yang C, *et al*. Enterohepatic recirculation of bioactive ginger phytochemicals is associated with enhanced tumor growth-inhibitory activity of ginger extract. *Carcinogenesis* 2014;**35**:1320–9.
40. Mohammadi M, Li Y, Abebe DG, *et al*. Folate receptor targeted three-layered micelles and hydrogels for gene delivery to activated macrophages. *J Control Release* 2016;**244**:269–79.
41. Yi YS. Folate receptor-targeted diagnostics and therapeutics for inflammatory diseases. *Immune Netw* 2016;**16**:337–43.
42. Low PS, Henne WA, Doorneweerd DD. Discovery and development of folic-acid-based receptor targeting for imaging and therapy of cancer and inflammatory diseases. *Acc Chem Res* 2008;**41**:120–9.
43. Zheng M, Zhao P, Luo Z, *et al*. Robust ICG theranostic nanoparticles for folate targeted cancer imaging and highly effective photothermal therapy. *ACS Appl Mater Interfaces* 2014;**6**:6709–16.
44. Seril DN, Liao J, Yang GY, Yang CS. Oxidative stress and ulcerative colitis-associated carcinogenesis: studies in humans and animal models. *Carcinogenesis* 2003;**24**:353–62.
45. Chassaing B, Aitken JD, Malleshappa M, Vijay-Kumar M. Dextran sulfate sodium [DSS]-induced colitis in mice. *Curr Protoc Immunol* 2014;**104**:Unit 15.25.
46. Chassaing B, Srinivasan G, Delgado MA, Young AN, Gewirtz AT, Vijay-Kumar M. Fecal lipocalin 2, a sensitive and broadly dynamic non-invasive biomarker for intestinal inflammation. *PLoS One* 2012;**7**:e44328.
47. Zschiebsch K, Fischer C, Pickert G, *et al*. Tetrahydrobiopterin attenuates DSS-evoked colitis in mice by rebalancing redox and lipid signalling. *J Crohns Colitis* 2016;**10**:965–78.
48. Veziant J, Gagnière J, Jouberton E, *et al*. Association of colorectal cancer with pathogenic *Escherichia coli*: focus on mechanisms using optical imaging. *World J Clin Oncol* 2016;**7**:293–301.
49. Dignass AU. Mechanisms and modulation of intestinal epithelial repair. *Inflamm Bowel Dis* 2001;**7**:68–77.
50. Makhlof A, Tozuka Y, Takeuchi H. pH-Sensitive nanospheres for colon-specific drug delivery in experimentally induced colitis rat model. *Eur J Pharm Biopharm* 2009;**72**:1–8.
51. Cheng G, An F, Zou MJ, Sun J, Hao XH, He YX. Time- and pH-dependent colon-specific drug delivery for orally administered diclofenac sodium and 5-aminosalicylic acid. *World J Gastroenterol* 2004;**10**:1769–74.
52. Ali H, Weigmann B, Collnot EM, Khan SA, Windbergs M, Lehr CM. Budesonide loaded PLGA nanoparticles for targeting the inflamed intestinal mucosa – pharmaceutical characterisation and fluorescence imaging. *Pharm Res* 2016;**33**:1085–92.
53. Frede A, Neuhaus B, Klopfleisch R, *et al*. Colonic gene silencing using siRNA-loaded calcium phosphate/PLGA nanoparticles ameliorates intestinal inflammation in vivo. *J Control Release* 2016;**222**:86–96.
54. Patil YB, Toti US, Khdair A, Ma L, Panyam J. Single-step surface functionalisation of polymeric nanoparticles for targeted drug delivery. *Biomaterials* 2009;**30**:859–66.
55. Toti US, Guru BR, Grill AE, Panyam J. Interfacial activity assisted surface functionalisation: a novel approach to incorporate maleimide functional groups and cRGD peptide on polymeric nanoparticles for targeted drug delivery. *Mol Pharm* 2010;**7**:1108–17.
56. Srivastava KC, Mustafa T. Ginger [*Zingiber officinale*] in rheumatism and musculoskeletal disorders. *Med Hypotheses* 1992;**39**:342–8.
57. Mashhadi NS, Ghiasvand R, Askari G, Hariri M, Darvishi L, Mofid MR. Anti-oxidative and anti-inflammatory effects of ginger in health and physical activity: review of current evidence. *Int J Prev Med* 2013;**4**:S36–42.
58. Luettig J, Rosenthal R, Lee IM, Krug SM, Schulzke JD. The ginger component 6-shogaol prevents TNF-α-induced barrier loss via inhibition of PI3K/Akt and NF-κB signaling. *Mol Nutr Food Res* 2016;**60**:2576–86.
59. Pan MH, Hsieh MC, Hsu PC, *et al*. 6-Shogaol suppressed lipopolysaccharide-induced up-expression of iNOS and COX-2 in murine macrophages. *Mol Nutr Food Res* 2008;**52**:1467–77.
60. Park G, Oh DS, Lee MG, Lee CE, Kim YU. 6-Shogaol, an active compound of ginger, alleviates allergic dermatitis-like skin lesions via cytokine inhibition by activating the Nrf2 pathway. *Toxicol Appl Pharmacol* 2016;**310**:51–9.
61. Chen H, Fu J, Chen H, *et al*. Ginger compound [6]-shogaol and its cysteine-conjugated metabolite [M2] activate Nrf2 in colon epithelial cells in vitro and in vivo. *Chem Res Toxicol* 2014;**27**:1575–85.
62. Mu J, Zhuang X, Wang Q, *et al*. Interspecies communication between plant and mouse gut host cells through edible plant derived exosome-like nanoparticles. *Mol Nutr Food Res* 2014;**58**:1561–73.
63. Baird L, Dinkova-Kostova AT. The cytoprotective role of the Keap1-Nrf2 pathway. *Arch Toxicol* 2011;**85**:241–72.
64. Feng J, Zhang P, Chen X, He G. PI3K and ERK/Nrf2 pathways are involved in oleanolic acid-induced heme oxygenase-1 expression in rat vascular smooth muscle cells. *J Cell Biochem* 2011;**112**:1524–31.
65. Na HK, Kim EH, Jung JH, Lee HH, Hyun JW, Surh YJ. [-]-Epigallocatechin gallate induces Nrf2-mediated antioxidant enzyme expression via activation of PI3K and ERK in human mammary epithelial cells. *Arch Biochem Biophys* 2008;**476**:171–7.
66. Lappas M, Permezel M, Georgiou HM, Rice GE. Nuclear factor kappa B regulation of proinflammatory cytokines in human gestational tissues in vitro. *Biol Reprod* 2002;**67**:668–73.
67. Park HJ, Kim IT, Won JH, *et al*. Anti-inflammatory activities of ent-16alphaH,17-hydroxy-kauran-19-oic acid isolated from the roots of Siegesbeckia pubescens are due to the inhibition of iNOS and COX-2 expression in RAW 264.7 macrophages via NF-kappaB inactivation. *Eur J Pharmacol* 2007;**558**:185–93.